J. Biochem. **138**, 183–191 (2005)
DOI: 10.1093/jb/mvi112

Expression of Functional *Streptomyces coelicolor* H$^+$-Pyrophosphatase and Characterization of Its Molecular Properties

Megumi Hirono, Hisatoshi Mimura, Yoichi Nakanishi and Masayoshi Maeshima*

Laboratory of Cell Dynamics, Graduate School of Bioagricultural Sciences, Nagoya University, Nagoya 464-8601

Received April 20, 2005; accepted May 24, 2005

H$^+$-translocating pyrophosphatases (H$^+$-PPases) are proton pumps that are found in many organisms, including plants, bacteria and protozoa. *Streptomyces coelicolor* is a soil bacterium that produces several useful antibiotics. Here we investigated the properties of the H$^+$-PPase of *S. coelicolor* by expressing a synthetic DNA encoding the amino-acid sequence of the H$^+$-PPase in *Escherichia coli*. The H$^+$-PPase from *E. coli* membranes was active at a relatively high pH, stable up to 50°C, and sensitive to *N*-ethylmaleimide, *N,N′*-dicyclohexylcarbodiimide and acylspermidine. Enzyme activity increased by 60% in the presence of 120 mM K$^+$, which was less than the stimulation observed with plant vacuolar H$^+$-PPases (type I). Substitutions of Lys-507 in the Gly-Gln-x-x-(Ala/Lys)-Ala motif, which is thought to determine the K$^+$ requirement of H$^+$-PPases, did not alter its K$^+$ dependence, suggesting that other residues control this feature of the *S. coelicolor* enzyme. The H$^+$-PPase was detected during early growth and was present mainly on the plasma membrane and to a lesser extent on intracellular membranous structures.

Key words: H$^+$-pyrophosphatase, proton pump, *Streptomyces coelicolor*.

Abbreviations: DCCD, *N,N′*-dicyclohexylcarbodiimide; H$^+$-PPase, H$^+$-pyrophosphatase; MEGA-9, *N*-nonanoyl-*N*-methylglucamine; NEM, *N*-ethylmaleimide; PP_i, inorganic pyrophosphatase; ScPP, H$^+$-PPase of *Streptomyces coelicolor*.

Proton pumps have two physiological roles: pH regulation and the formation of proton-motive forces across membranes. They convert the energy of chemical bonds into the active transport of H$^+$. The simplest of these pumps is the H$^+$-translocating inorganic pyrophosphatase (H$^+$-PPase), which consists of a single polypeptide of about 80 kDa (*1*). H$^+$-PPases are found in plants, parasitic and free-living protozoa, and some eubacteria and archaebacteria (*2–8*). Recently, an H$^+$-PPase was detected in membranes of the ovary and egg yolk granules of the insect *Rhodnius prolixus* (*9*). In prokaryotes such as *Rhodospirillum rubrum* (*10*) and *Agrobacterium tumefaciens* (*11*), the enzyme generates a proton gradient across the plasma membrane and the membranes of acidocalcisomes.

H$^+$-PPases are excellent models for research on the coupling between PPi hydrolysis and active H$^+$ transport, and their structure–function relationships have been investigated extensively (*4*, *12–17*). Studies using heterologous-expression systems to analyse mutant forms of these enzymes have revealed their membrane topology and identified several functional motifs. They are divided into two groups according to their K$^+$ requirements: one requires K$^+$ for maximal activity (*1*), whereas the other does not (*4*, *5*). The former is designated type I and the latter is known as type II (*4*, *5*).

Streptomyces coelicolor is a bacterium (*Actinomycetes*) that produces most of the natural antibiotics used in human and veterinary medicine. Its H$^+$-PPase (ScPP) was identified by genome sequencing (*18*). *S. coelicolor* is phylogenetically distant from other organisms with H$^+$-PPases, and the physiological role of its H$^+$-PPase is not known. In the present study, we detected ScPP in *S. coelicolor* cells, expressed it in *E. coli* and determined its biochemical properties. We focused particularly on its K$^+$ dependence, as this property distinguishes the two types of H$^+$-PPase (*4*, *5*). We also examined the K$^+$ dependence of mutant forms of ScPP.

MATERIALS AND METHODS

Synthesis of DNA Encoding ScPP and Expression in E. coli—A laboratory strain of *S. coelicolor* cells was cultivated on agar plates containing 0.1% yeast extract, 0.1% beef extract, 0.2% Nzamine, 1% glucose and 2% agar at 30°C. DNA was isolated according to standard procedures, and was used as a template to amplify the DNA encoding the H$^+$-PPase by PCR with a pair of forward and reverse primers. We found that the nucleotide sequence of the native gene for H$^+$-PPase (DDBJ/GenBank^{TM}/EBI Data Bank accession no. AB180905) differed by eight bases from the reported sequence: T/C845, C/G921, G/A1149, T/C1593, G/A1803, G/A1833, G/A1884 and T/C2049 (reported sequence/results of the present study; numbered from the open reading frame specifying 794 amino acids). The deduced amino-acid sequence agreed with that in the database (*18*) (DDBJ/GenBank^{TM}/EBI accession no. AL645882), with the exception of Phe^{282} (Ser in the database). We designed and synthesized an artificial ScPP DNA (*sScPP*) with a gene synthesizer program (MacPerl Script) coding for the same amino-acid sequence as the native H$^+$-PPase. A plasmid, pYN309,

*To whom correspondence should be addressed.Tel/Fax: +81-52-789-4096, E-mail: maeshima@agr.nagoya-u.ac.jp

derived from pET23b (Novagen) by modifying the *Pst*I site, was used for expressing the ScPP proteins. A His_6 tag was added to the carboxyl (C)-terminus to facilitate purification of the ScPP protein. The *ScPP* DNA construct was introduced into *E. coli* strain BL21(DE3)pLysS (Novagen), and transformants were selected for antibiotic resistance on Luria-Bertani plates containing 50 mg·liter^{-1} of spectinomycin and 30 mg·liter^{-1} of kanamycin. The constructs for generating the mutant ScPPs were prepared as described previously (*15*).

Preparation of E. coli Membranes—*E. coli* cells expressing ScPP were grown with antibiotics on Luria-Bertani plates. After 4 h at 37°C (OD_{660} = 0.7), isopropyl-1-thio-β-D-galactopyranoside was added to a final concentration of 0.4 mM. The cells were incubated for a further 2 h, harvested by centrifugation at 3,500 × *g* for 10 min, and suspended in 50 mM Tris-Mes (pH 7.3), 1 mM EGTA, 2 mM DTT, 75 mM KCl, 0.15 M sucrose and 1 mM PMSF. They were incubated with 40 mg·liter^{-1} DNase I and 0.2 g·liter^{-1} lysozyme at 4°C for 10 min, then thoroughly disrupted with a bath-type sonicator (Cosmobio Co., Japan). The homogenate was centrifuged at 2,000 × *g* for 10 min, and the supernatant was further centrifuged at 150,000 × *g* for 20 min. The resulting pellet was suspended in 10 mM Tris-Mes (pH 7.3), 1 mM $MgCl_2$, 1 mM DTT, 100 mM KCl, 0.15 M sucrose and 0.5 mM PMSF and used as the *E. coli* membrane fraction.

Solubilization and Purification of ScPP—Sucrose monocholate at a final concentration of 2% (w/v) was added to the *E. coli* membrane fraction (2.0 g·liter^{-1}), and the suspension was stirred at 25°C for 30 min, sonicated for 2 min and centrifuged at 100,000 × *g* for 30 min. The supernatant was mixed with *E. coli* total lipid extract to a final concentration of 0.20 mg·ml^{-1} and applied to a column (bed volume = 4 ml) of Q-Sepharose (Amersham Biosciences) equilibrated with 20 mM Tris-HCl (pH 7.5), 0.15 M sucrose, 2 mM $MgCl_2$, 1% sucrose monocholate (Dojin Chemicals), 100 mM KCl and 0.2 mg·ml^{-1} *E. coli* total lipid extract (buffer B). ScPP was eluted from the column with 10 ml of buffer B containing 200 mM NaCl (buffer C) and applied to a column (bed volume = 2 ml) of Ni-Sepharose (Amersham Biosciences) pre-equilibrated with buffer C. The column was washed with 10 ml of buffer C containing 30 mM imidazole, and ScPP was eluted with 5 ml of buffer C containing 150 mM imidazole and stored at –80°C. All purification steps were performed at 0–4°C.

Enzyme Assay—PP_i hydrolysis was assayed as described previously (*7*) with a few modifications. The standard reaction medium contained 20 mM Bicine-NaOH (pH 8.0), 100 mM KCl, 1 mM $MgCl_2$, 0.15 M sucrose, 0.4 mM Na_4PP_i, 1 mM sodium molybdate and 0.5 mM NaF. The reaction was carried out at 30°C. PP_i-dependent H^+-transport activity was measured at 25°C as the rate of fluorescence quenching of fluorescent monoamine acridine orange (*7*). Membrane preparations were preincubated with the standard reaction buffer containing 20 mM Bicine-NaOH (pH 8.0), 100 mM KCl, 1 mM $MgCl_2$, 0.15 M sucrose, and 0.75 μM acridine orange, and the reaction was initiated by the addition of 0.4 mM Na_4PPi at 25°C.

Extraction of Protein from S. coelicolor Cells—*S. coelicolor* was cultivated at 30°C in Bennet medium containing 0.1% yeast extract, 0.1% beef extract, 0.2% Nzamine, 1% glucose and 2% agarose. Cells grown for two, four, and six days were treated with 10% SDS and centrifuged at 5,000 × *g* for 20 min. The supernatants were collected and used as *S. coelicolor* protein extracts. In some experiments, *S. coelicolor* was cultivated at 30°C in S2 liquid medium containing 1% galactose, 1% dextrin, 0.5% soyton, 0.1% $(NH_4)_2SO_4$ and 0.12% $CaCO_3$ (pH 7.4).

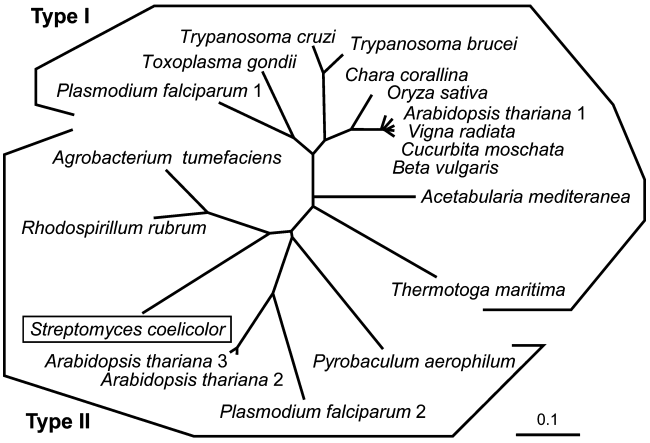

Fig. 1. **Phylogenetic analysis of the H^+-PPases of *S. coelicolor*, and selected prokaryotes and eukaryotes.** The tree was constructed from alignments of full-length amino-acid sequences using Clustal W and TreeView. The enzymes are designated as type I or II H^+-PPases on the basis of previous reports (*4*, *5*). The accession numbers for the sequences used are: *Arabidopsis thaliana* 1 (DDBJ/GenBank™/EBI protein ID, BAA32210), *A. thaliana* 2 (BAA92151), *A. thaliana* 3 (AAG09080), *Vigna radiata* (BAA23649), *Oryza sativa* (BAA08232), *Beta vulgaris* (AAA61609), *Cucurbita moschata* (BAA33149), *Chara corallina* (BAA36841), *Acetabularia mediterranea* (BAA83103), *Plasmodium falciparum* 1 (AAD17215), *P. falciparum* 2 (AAG21366), *Toxoplasma gondii* (AAK38076), *T. cruzi* (AAF80381), *T. brucei* (AAK95376), *R. rubrum* (AAC38615), *S. coelicolor* (CAB38484), *Thermotoga maritima* (AAD35267), *A. tumefaciens* (AAK86977) and *P. aerophilum* (AAF01029). The scale bar of 0.10 is equal to 10% sequence divergence.

SDS-PAGE and Immunoblotting—Proteins were separated by SDS-PAGE on 12.5% gels and transferred to a PVDF membrane using the standard procedure. Immunoblotting was carried out with polyclonal antibodies against a synthetic peptide, DVGADLVGKVEC, corresponding to the conserved catalytic motif of H^+-PPases (*20*), together with horseradish peroxidase–linked protein A and ECL Western blotting detection reagents (Amersham Biosciences).

Electron Microscopy and Immunocytochemical Analysis—*S. coelicolor* was cultivated at 30°C for two days in Bennet medium, and the cells were incubated in 2% glutaraldehyde for 15 h and in osmium tetroxide for 3 h. After dehydration in ethanol, they were embedded in EPON812. Ultra-thin sections (thickness = 80 nm) were prepared with an ultramicrotome, mounted on uncoated nickel grids, and labeled with anti H^+-PPase antibody and protein A-gold (diameter = 10 nm).

RESULTS

Expression of ScPP in E. coli and Its Purification—As shown in the phylogenetic tree of H^+-PPases (Fig. 1), ScPP is relatively distant from the well-characterized H^+-

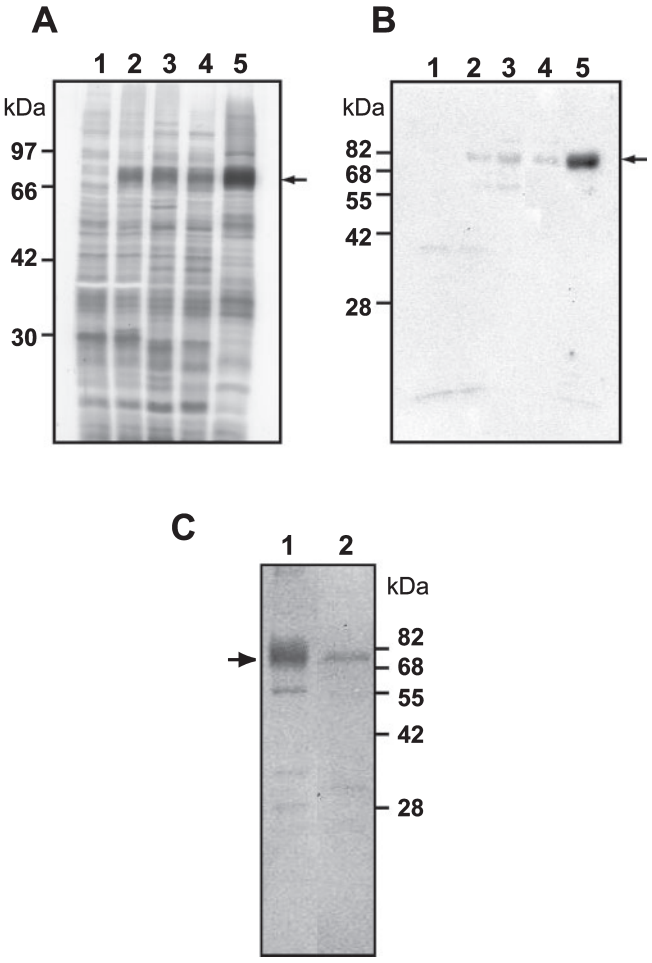

Fig. 2. **Expression of ScPP in *E. coli*.** DNA encoding *S. coelicolor* ScPP was introduced into *E. coli* cells and expressed by adding IPTG. To detect the expressed ScPP, SDS-PAGE gels were subjected to silver-staining (A) and immunoblotted with the antibody to H⁺-PPase (B). Lane 1, membrane fraction from control *E. coli* cells with vacant vector; lane 2, membranes from *E. coli* expressing ScPP; lane 3, solubilized fraction of H⁺-PPase–containing membranes; lane 4, 200 mM NaCl eluate from a Q-Sepharose column; lane 5, eluate from a Ni-Sepharose column. A 2-μg sample of protein was applied to each lane. Arrows indicate the position of ScPP. (C) Immunoblot analysis of membrane preparations (10 μg) from *E. coli* expressing ScPP (lane 1) and from *S. coelicolor* cells (lane 2).

PPases of other organisms, including plants (*1*, *5*), *R. rubrum* (*3*, *10*), *Trypanosoma cruzi* (*8*), *Trypanosoma brucei* (*19*) and *A. tumefaciens* (*11*). It contains 794 amino-acid residues and a characteristic long additional carboxyl-terminal sequence that includes a transmembrane domain (*15*).

Expression of ScPP in *E. coli* was confirmed by immunoblotting with an anti–H⁺-PPase antibody raised against the conserved motif of H⁺-PPase (Fig. 2) (*20*). The expressed ScPP constituted only a few percent of the total membrane protein of the transformants, as judged by SDS-PAGE (Fig. 2A, lane 2). The membrane-associated PP_i-hydrolyzing activity was approximately 100 nmol $PP_i \cdot min^{-1} \cdot mg^{-1}$ at 30°C in an assay medium containing sodium fluoride, which inhibited soluble PPases. PP_i-dependent H⁺-transport was also observed (see below).

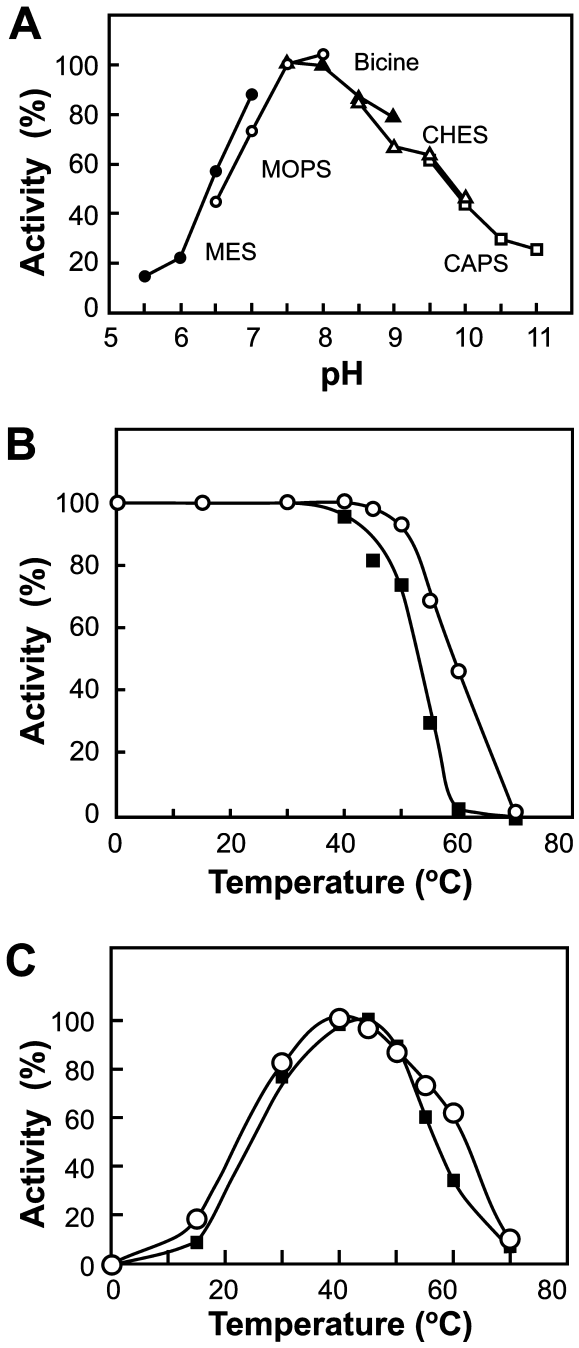

Fig. 3. **The pH and temperature dependence of ScPP.** (A) The membrane fraction from recombinant *E. coli* cells was assayed for PP_i-hydrolyzing activity in the following buffers: MES (closed circles), MOPS (open circles), BICINE (closed triangles), CHES (open triangles) and CAPS (open squares). (B) Membrane-bound (open circles) and partially purified ScPP (closed squares) were assayed at 30°C after incubation at the indicated temperatures for 30 min in the presence of 1 mM $MgCl_2$. (C) Membrane-bound (open circles) and partially purified ScPP (closed circles) were assayed at the indicated temperatures for 30 min. Activity is expressed as a percentage of the maximal activity in each experiment.

Control membranes had little hydrolyzing activity and showed no PP_i-dependent H⁺-transport.

To solubilize the membrane-bound ScPP, we tested various concentrations of 20 different detergents includ-

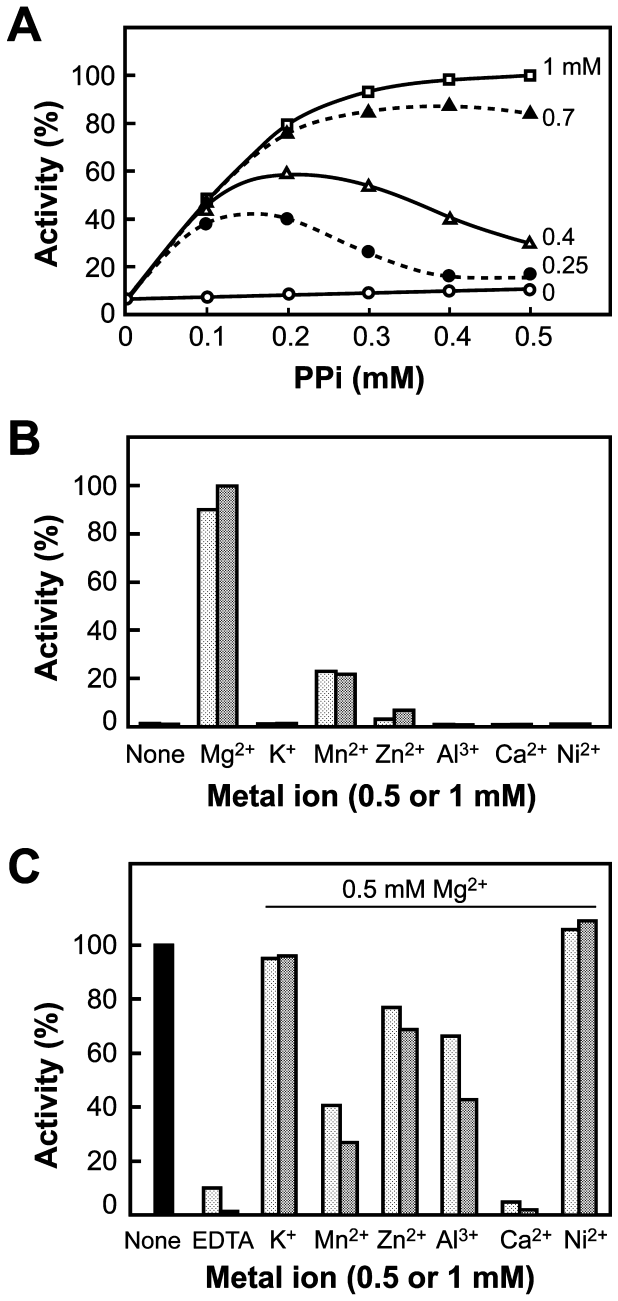

Fig. 4. **Effect of metal ions on the PPase activity of ScPP.** (A) The PPase activity of the membrane fraction was measured in a standard assay mixture containing the indicated concentrations of Mg^{2+} and PP_i. Values are expressed relative to activity at 1 mM Mg^{2+} and 0.5 mM PP_i. (B) The activity of the membrane fraction was assayed in the presence of Mg^{2+} and other metal ions at 0.5 mM (light-shaded bars) or 1 mM (shaded bars). Activity is expressed relative to that with 1 mM Mg^{2+}. (C) Activity was assayed in the presence of 0.5 mM Mg^{2+} plus the indicated metal ion at 0.5 mM (light-shaded bars) or 1 mM (shaded bars). Activity is expressed relative to the control activity in the presence of 0.5 mM Mg^{2+} (closed bar). Activity is expressed as a percentage of the maximal activity in the presence of 1 mM Mg^{2+} (approximately 120 nmol $PP_i \cdot min^{-1} \cdot mg^{-1}$) in each experiment.

ing *n*-dodecyl-β-D-maltoside, sucrose monolaurate, *N*-nonanoyl-*N*-methylglucamine (MEGA-9), lysolecithin and zwittergent. Most detergents inactivated the enzyme, and only sucrose monocholate solubilized it in an active form with good recovery. Thus, the enzyme was routinely solubilized with 1% sucrose monocholate in the presence of 2 mM $MgCl_2$ and 100 mM KCl, and the recovery was 20%. The solubilized fraction was further purified by Q-Sepharose and Ni-Sepharose chromatography, and ScPP was detected by immunoblotting (Fig. 2B). The recombinant enzyme with a His_6 tag was partially purified, and its specific activity was several-fold greater than that of the original membrane preparation. Addition of a His_6 tag had no effect on the enzyme activity, as described previously (*15*). The PP_i-hydrolysis activity was approximately 450 nmol $PP_i \cdot min^{-1} \cdot mg^{-1}$ at 30°C and required phospholipid micelles (data not shown), similarly to plant vacuolar H^+-PPase (*7*).

Effects of pH and Temperature on the Activity and Stability of ScPP—Figure 3A shows the pH dependence of PP_i hydrolysis. As the crude *E. coli* membrane preparation contained a relatively high level of soluble PPase activity, the membranes were assayed in the presence of NaF, which is a potent inhibitor of soluble PPases. ScPP had maximal activity at pH 7.5–8.0. Purified mung bean vacuolar H^+-PPase has an optimum pH of 7.0 and expresses only 20% of the maximum activity at pH 6.0 and 8.0 (data not shown). The apparent K_m values for PP_i of the membrane-bound ScPP and the partially purified preparation were 110 μM and 120 μM, respectively. The calculated K_m of ScPP for its actual substrate, Mg_2PP_i, was about 3.5 μM; this was comparable to that of the mung bean enzyme (*21*).

Membrane-bound ScPP retained full activity after incubation at 50°C for 30 min, and the purified enzyme retained 70% of its activity under the same conditions (Fig. 3B). It should be noted that ScPP activity was only stable in the presence of 1 mM Mg^{2+}. The optimum temperature for PP_i-hydrolysis was 40–45°C for both the membranous and purified preparations (Fig. 3C).

Requirement of K^+ for ScPP Activity—Figure 4A shows the substrate-activity curves at various concentrations of Mg^{2+}. The enzyme had a strict requirement for Mg^{2+}, and maximal activity was obtained in the presence of 1 mM Mg^{2+} and more than 0.4 mM PP_i. This is also true of H^+-PPases in general (*7*, *22*). As shown in Fig. 4B, the most effective metal ion was Mg^{2+}, although Mn^{2+} could act as a partial substitute. The enzyme was strongly inhibited by Ca^{2+} at 0.5 mM (Fig. 4C), and Mn^{2+}, Zn^{2+} and Al^{3+} were partially inhibitory at 0.5 mM. Although Ni^{2+} did not inhibit the enzyme, it could not substitute for Mg^{2+}.

The requirement of K^+ for activity is thought to be a key property distinguishing type I and II H^+-PPases (*4*). KCl at relatively high concentrations (120 mM) enhanced PPi-hydrolysis in both the membrane and the partially purified ScPP fractions (Fig. 5, A and D). A similar effect was observed with CH_3COOK (Fig. 5B), but not with NaCl (Fig. 5C). Thus, the stimulation was due to K^+ itself. However, the extent of the stimulation was low (60%) compared with the plant vacuolar H^+-PPases, the activity of which was increased by more than three-fold (*7*, *23*). As shown in Fig. 5E, the rubidium ion, which is substituted for K^+ in experiments on K^+ channels, stimulated the activity as effectively as K^+.

Tris has been reported to act as a competitive inhibitor of K^+ that represses plant vacuolar H^+-PPases at more

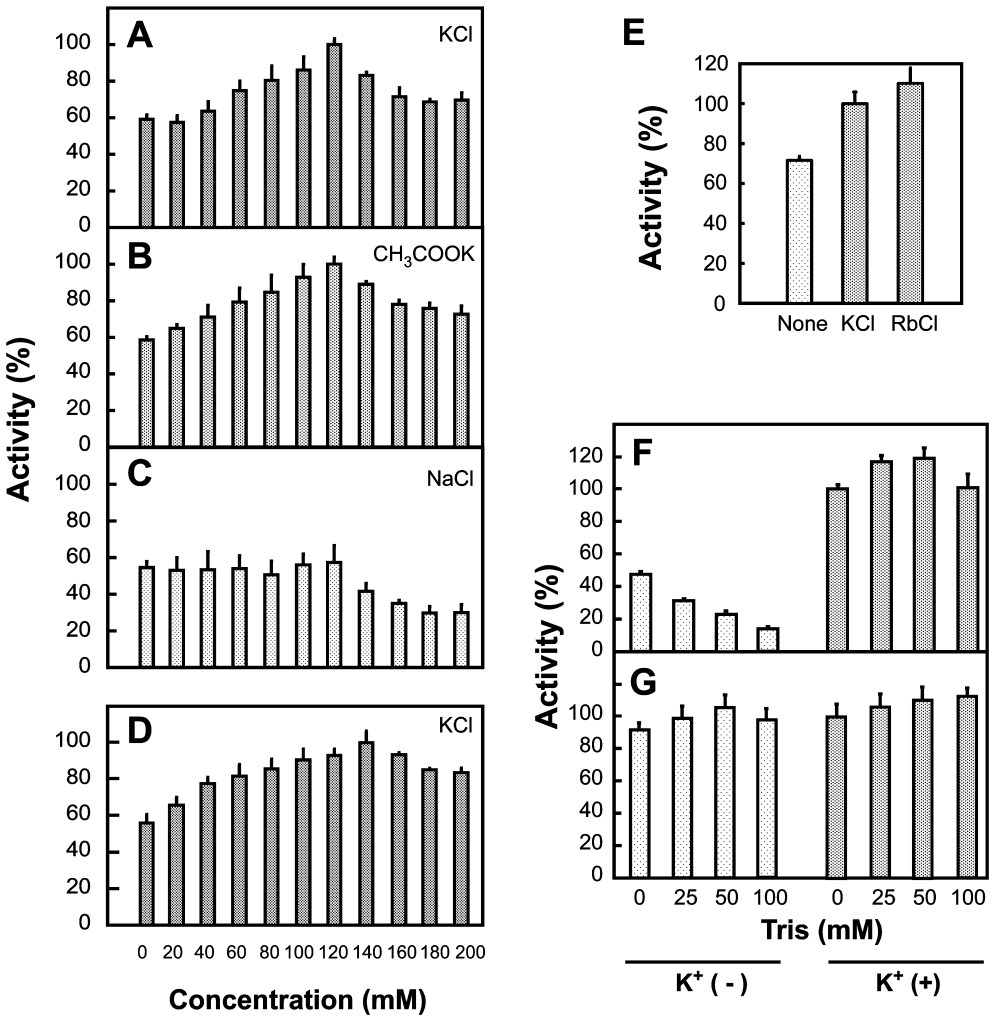

Fig. 5. **Limited dependence of the PPase activity of ScPP on K⁺.** PP_i hydrolysis by the membrane fraction was assayed in the presence of the indicated concentrations of KCl (A), CH_3COOK (B) and NaCl (C). The partially purified enzyme was assayed for H⁺-PPase activity at various KCl concentrations (D). Activity is expressed relative to that in 120 mM KCl (A–C) or 140 mM KCl (D). Membrane-bound ScPP was assayed for PPase activity in the presence of 100 mM KCl or RbCl (E). Mung bean vacuolar membranes (F) and *E. coli* membranes (G) containing ScPP were assayed for PPase activity in the presence of the indicated concentrations of Tris and in the presence (+) or absence (−) of 50 mM KCl. PPase activity is expressed relative to that in 50 mM KCl without Tris.

than 25 mM (*24*). Indeed, Tris markedly inhibited mung bean vacuolar H⁺-PPase in the absence of KCl, and the effect was reversed by KCl (Fig. 5F). By contrast, the activity of ScPP was not inhibited by Tris in either the presence or absence of KCl. This appears to be a characteristic of ScPP.

The stimulation of PP_i-dependent H⁺-transport activity was also examined using an acridine orange fluorescence-quenching assay (Fig. 6A). The initial rate of fluorescence quenching was stimulated six-fold by adding 100 mM KCl (Fig. 6B), and RbCl at 100 mM had a similar effect (Fig. 6C). However, NaCl also stimulated pump activity (Fig. 6B).

H⁺-PPases that do not require K⁺ for their activity are classified as type II and are thought to depend on the GNxxKA motif (*4*) in the conserved cytoplasmic loop between the eleventh and twelfth transmembrane domains. The limited dependence of ScPP on K⁺ suggests that it is a type II enzyme. We therefore generated mutant enzymes with Lys-507 substituted by Ala (K507A) or Arg (K507R). The mutant enzymes were expressed well in *E. coli* (Fig. 7A), and the amino-acid substitutions resulted in reduced activity, suggesting that this motif is, indeed, involved in catalysis (Fig. 7B). It should be noted that these substitutions of the lysine residue did not affect the K⁺-dependence of ScPP. It has been reported that the threonine residue close to this motif is also essential for K⁺-independence (*4*, *5*). However, neither a single (T510G) nor a double (K507A/T510G) mutation involving this site altered the K⁺ dependence.

Sensitivity of ScPP to Inhibitors—ScPP was sensitive to the substrate analogue imidodiphosphate, the proton-transport blocker *N,N′*-dicyclohexylcarbodiimide (DCCD) (*7*), the sulfhydryl agent *N*-ethylmaleimide (NEM) and acylspermidine D (Fig. 8). The K_i of imidodiphosphate was 50 μM (Fig. 8A), which was comparable to the reported value for mung bean H⁺-PPase (apparent K_i = 12 μM) (*25*). DCCD, which reacts with carboxyl groups in hydrophobic regions, has been reported to bind and inhibit H⁺-PPases (*7*, *26*, *27*). The K_i of DCCD for ScPP (0.2 mM) (Fig. 8B) was similar to that for plant H⁺-PPase (0.5 mM) (*7*). The K_i of NEM was 3 μM (Fig. 8C), which was similar to that of the *Arabidopsis* enzyme (*13*). The K_i of acylspermidine D from soft coral (*28*) was 3 $\mu g \cdot ml^{-1}$ (Fig. 8D), which was comparable to that for mung bean H⁺-PPase (6 $mg \cdot ml^{-1}$) (*28*). These results indicate that the fundamental structural and functional characteristics of H⁺-PPases are conserved in ScPP.

Detection of ScPP in S. coelicolor Cells—To determine whether ScPP protein could be detected in *S. coelicolor* cells, we obtained crude membrane preparations from

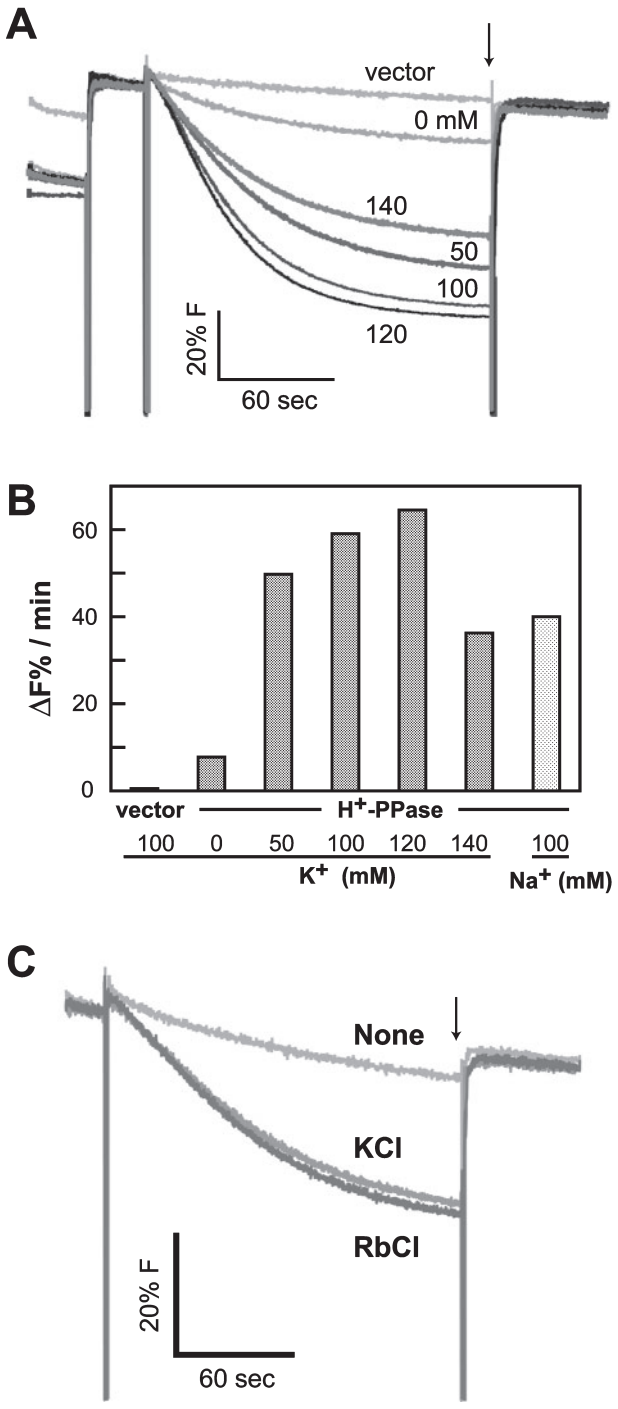

Fig. 6. **Metal ion dependence of the proton-pump activity of ScPP.** Membrane vesicles were prepared from ScPP-expressing *E. coli* cells and assayed for PP_i-dependent proton pumping in the presence of various concentrations of KCl. (A) Fluorescence quenching of acridine orange recorded with a fluorescence spectrophotometer. Ammonium chloride was added to collapse the proton gradient generated by the H^+-PPase at the indicated time points (arrows). (B) Initial rates of fluorescence quenching in the presence of various metal ion concentrations. (C) PP_i-dependent proton-pump activity in the presence of 100 mM KCl or RbCl under the same conditions.

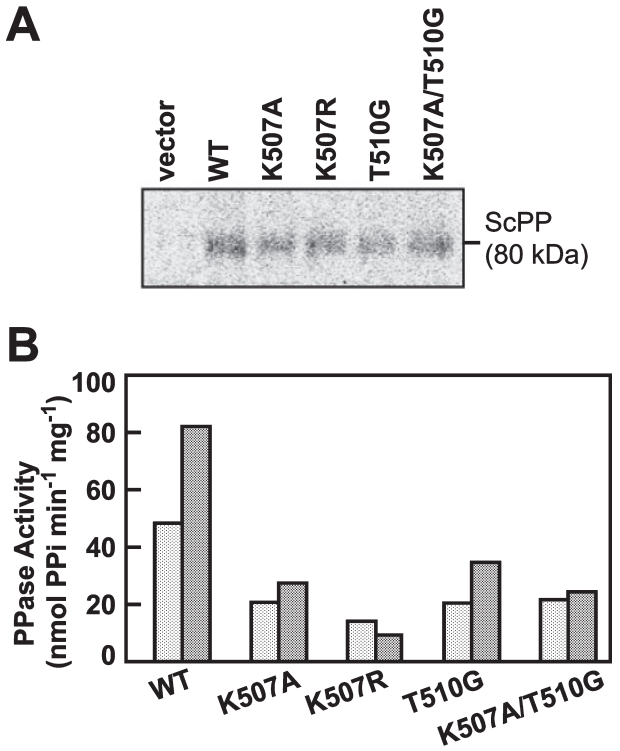

Fig. 7. **Dependence of ScPP mutants on K^+.** (A) Wild-type and mutant enzymes (K507A, K507R, T510G and K507A/T510G) were expressed in *E. coli*, and gels of the membrane fractions (10 μg) were immunoblotted with anti–H^+-PPase antibody. ScPP was located at a position corresponding to 80 kDa. (B) *E. coli* membranes containing WT and mutant enzymes were assayed for PPase activity in the presence (shaded bars) or absence (light-shaded bars) of 120 mM KCl. The data are presented as the mean of five experiments.

relatively young cells and subjected them to immunoblotting. ScPP protein was clearly detected at approximately 70 kDa in membranes prepared from 2-day-old cultures. The protein had decreased by day 4 and had disappeared by day 6 (Fig. 9, A and B). The 70-kDa protein was not a major component of the crude membrane fraction, as shown by a Coomassie Blue–stained SDS-PAGE gel. Therefore, the H^+-PPase might be a minor component of *S. coelicolor* membranes. Electron-microscopic images revealed membranous structures in the cells cultured for two days (Fig. 9, C and D). We carried out an immunocytochemical analysis to determine the intracellular location of the ScPP. Numerous protein A-gold particles that reacted with the antibody were located in the plasma membrane (Fig. 10). There were also some particles in the cell interiors.

DISCUSSION

In this study, we characterized the ScPP of *S. coelicolor*, the primary structure of which is phylogenetically distant from the H^+-PPases of other organisms (Fig. 1). The growth rate of *S. coelicolor* is relatively low, and the H^+-PPase activity of the crude membrane fraction (approximately 7.0 $nmol \cdot min^{-1} \cdot mg^{-1}$) was much lower than in the vacuolar membranes of young plants (1,100 $nmol \cdot min^{-1} \cdot mg^{-1}$) (7). We therefore expressed ScPP in *E.*

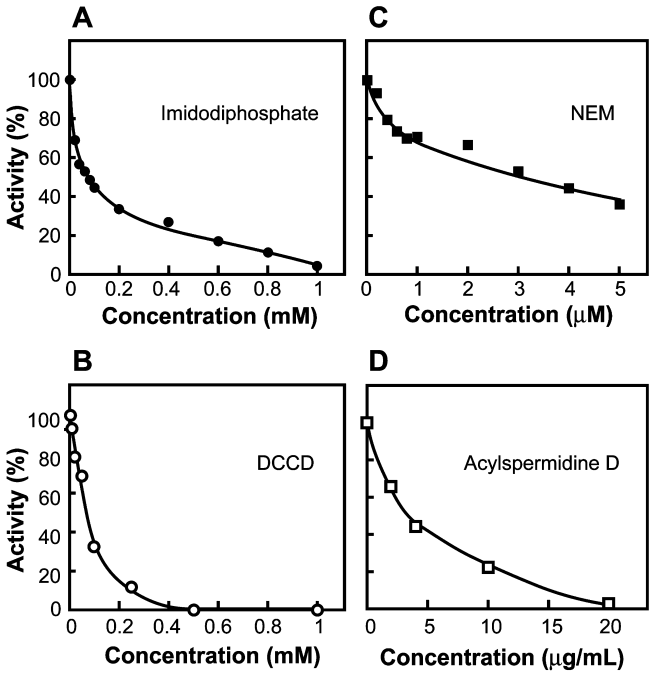

Fig. 8. **Inhibitory effect of imidodiphosphate, a PP_i analogue, and other inhibitors on PPase activity.** Membrane vesicles were assayed for PP_i hydrolysis in the standard assay medium in the presence of the indicated concentrations of imidodiphosphate (A), DCCD (B), NEM (C) and acylspermidine D (D).

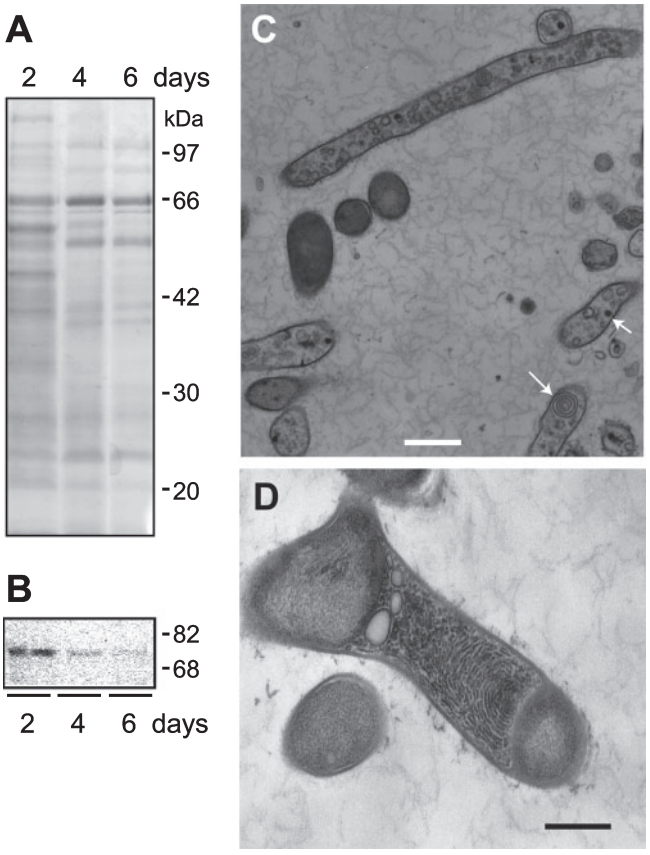

Fig. 9. **Detection of H⁺-PPase in *S. coelicolor* cells.** Membranes were prepared from *S. coelicolor* cells cultivated on agarose plates for 2, 4 and 6 days, and aliquots (28 μg) were subjected to SDS-PAGE, stained with Coomassie Blue (A) and immunoblotted with anti–H⁺-PPase antibodies (B). Electron micrographs of cells of *S. coelicolor* (C and D). Cells cultivated for two days were fixed as described in "MATERIALS AND METHODS." Arrows indicates intracellular structures. Scale bars = 1 μm (C) and 500 nm (D).

coli, where it could be partially purified from membranes (Figs. 2, 3 and 6).

Biochemical Characteristics of ScPP—Several parameters of ScPP—such as its requirement for phospholipids and Mg^{2+}, inhibition by Ca^{2+}, and the apparent K_m values for PP_i and Mg_2PP_i (Figs. 4 and 8)—are similar to those of other H⁺-PPases (*1*). Its thermal stability is higher than that of a purified plant enzyme that was completely inactivated at 40°C (*29*), but lower than that of the enzyme of *Pyrobaculum aerophilum*, which had maximal activity at 80°C when expressed in yeast (*30*). The thermal stability of H⁺-PPases is likely to depend on the structure of both the transmembrane domains and the catalytic domain formed by the cytoplasmic loops. Future studies of the three-dimensional structures of H⁺-PPases should provide insight into the basis of their thermal stabilities.

H⁺-PPases are divided into types I and II according to their requirement for K^+ (*5*). It has been proposed that the presence of a lysine versus an alanine residue in the conserved GNxx(A/K)A motif of one of the cytoplasmic segments distinguishes the two types (*4*). This motif is located in the cytoplasmic loop between the eleventh and twelfth transmembrane domains of ScPP. According to this criterion, ScPP is a type II enzyme, as it has the sequence GNTTKA (residues 503-508) (*15*).

In general, type I plant vacuolar H⁺-PPases are stimulated more than four-fold by K^+ (*23*, *31*), whereas ScPP was only slightly stimulated (Fig. 5). Therefore, both its relative lack of dependence on K^+ and the presence of a lysine residue (Lys-507) in the critical motif indicate that it is a type II H⁺-PPase. Although its H⁺-pump activity, unlike PP_i-hydrolysis, was strongly stimulated by 100 mM KCl, similar stimulation was obtained with NaCl or RbCl. This was probably due to the Cl^- ions, which act as counter ions during H^+ transport and can be replaced by other anions, such as sulphate (*32*). The transport of chloride ions might take place through a chloride channel, rather than *via* the H⁺-PPase itself.

The lack of dependence of ScPP on K^+ was further examined by making amino-acid substitutions (Fig. 7). The substitution of Lys-507, which is reported to be a key residue affecting K^+ dependence, did not alter this activity of ScPP. Similarly, the replacement of another potentially key residue, Thr-510 (T510G and K507A/T510G), did not increase the K^+ dependence. Therefore, the lysine and threonine residues in the conserved motif (GNTTKAIT; 503–510 in ScPP) do not control the K^+ dependence of ScPP. The other residues may determine this property with Lys-507 in the tertiary structure of the catalytic domain.

ScPP was inhibited by imidodiphosphate, DCCD, NEM and acylspermidine (Fig. 8). Its sensitivity to these inhibitors was similar to that of other H⁺-PPases, such as the *R. rubrum* enzyme (*10*). DCCD, which is an inhibitor of proton conductance, has been reported to react with Glu-

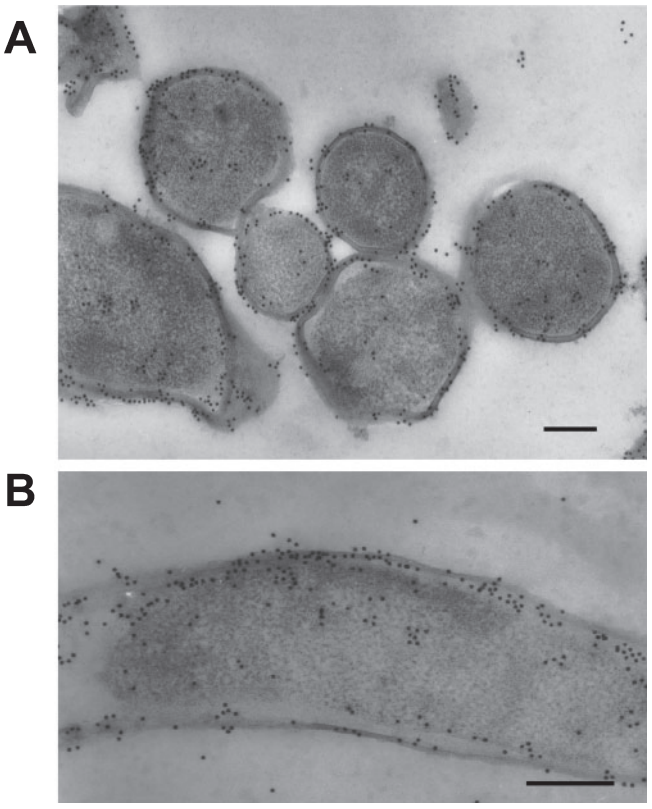

Fig. 10. **Immunogold labeling of H⁺-PPase.** Thin sections of *S. coelicolor* cells cultured for 2 days were treated with antibody to H⁺-PPase. Bound antibody was visualized with protein A coupled to 10 nm colloidal gold particles. Scale bar = 200 nm.

305 and Asp-504 of *Arabidopsis* H⁺-PPase (*27*). These residues correspond to Glu-262 and Asp-469 of ScPP, which are located in the sixth transmembrane domain and on the cytoplasmic side of the eleventh transmembrane domain, respectively (*15*). Therefore, these two residues, or the neighboring transmembrane domains (the sixth and eleventh), might be involved in H⁺ translocation.

The sulfhydryl reagent NEM reacts with Cys-634 of the *Arabidopsis* enzyme, which corresponds to Cys-621 of ScPP (*15*), and inhibits the enzyme (*25*). The amino-acid sequence of loop *m*, which includes Cys-621, is not conserved in H⁺-PPases. Acylspermidine derivatives isolated from a soft coral are novel inhibitors of plant vacuolar H⁺-PPase (*28*). They do not inhibit soluble-type PPase or the other proton pumps. Our findings support the theory that these compounds are useful for identifying type I and II H⁺-PPases, although their target site is unknown.

Presence of H⁺-PPase in S. coelicolor—ScPP protein could be detected by immunological methods, at least in the early stages of *S. coelicolor* growth (Figs. 9 and 10). Over a period of two days, germ tubes emerge from the spores and grow by tip extension and branch formation to form a mycelium extending into the medium. ScPP was observed mainly in the plasma membrane, but was also detected in intracellular membranous structures. During growth, *S. coelicolor* cells synthesize many kinds of macromolecules, including proteins, RNAs and cell wall components, and generate a large amount of PP_i as a byproduct, as do growing plant cells (*33*). ScPP might scavenge cytosolic PP_i to stimulate macromolecular biosyntheses. It might also generate a pH gradient across the plasma membrane to provide a driving force for secondary active-transport systems for the uptake of nutrients, the secretion of secondary metabolites and the release of waste products.

It should be noted that some membranous structures were observed in two-day-old cells of *S. coelicolor* (Fig. 9), and immunocytochemical analysis suggests that they contained ScPP (Fig. 10). Recently, Docampo and colleagues have demonstrated that H⁺-PPase is located in acidocalcisomes and related organelles in certain microorganisms (*8*, *10*, *11*, *34–36*). In the unicellular eukaryote *T. cruzi*, H⁺-PPase is located in the acidocalcisomes and contractile vacuoles and is thought to be involved in osmoregulation (*37*). H⁺-PPase was first described in the photosynthetic bacterium *R. rubrum* (*2*, *38*), where it was found on the chromatophore membrane that is continuous with the plasma membrane, and functions in the photophosphorylation of inorganic orthophosphate to pyrophosphate (*3*). However, this enzyme also exists in the membranes of the acidocalcisomes of *R. ruburum*, where it functions in the acidification of the intracellular compartment (*10*). The H⁺-PPase of the soil bacterium *A. tumefaciens* is also present in volutin granules, which resemble acidocalcisomes (*11*). In future studies, we intend to determine whether *S. coelicolor* possesses acidocalcisomes or similar structures. If it does, we will assess the relationship between these organelles and the intracellular membranous structures that were observed in young cells of *S. coelicolor* (Fig. 9). The function of these structures and the physiological role of ScPP remain to be determined.

This work was supported, in part, by Grants-in-Aid for Scientific Research from the Ministry of Education, Sports, Culture, Science and Technology of Japan to M.M. (nos. 16380068, 13CE2005 and 14COEA2). M.H. is a recipient of the Japan Society for the Promotion of Science for Young Scientists Research Fellowship 16–5967.

REFERENCES

1. Maeshima, M. (2000) Vacuolar H⁺-pyrophosphatase. *Biochim. Biophys. Acta* **1465**, 37–51
2. Baltscheffsky, H., von Steding, L.V., Heldt, H.W., and Klingenberg, M. (1966) Inorganic pyrophosphatase: formation in bacterial photophosphorylation. *Science* **153**, 1120–1122
3. Baltscheffsky, M., Schultz, A., and Baltscheffsky, H. (1999) H⁺-PPases: a tight membrane-bound family. *FEBS Lett.* **457**, 527–533
4. Belogurov, G.A. and Lahti, R. (2002) A lysine substitute for K⁺: A460K mutation eliminates K⁺ dependence in H⁺-pyrophosphatase of *Carboxydothermus hydrogenoformans*. *J. Biol. Chem.* **277**, 49651–49654
5. Drozdowicz, Y.M. and Rea, P.A. (2001) Vacuolar H⁺-pyrophosphatases: from the evolutionary backwaters into the mainstream. *Trends Plant Sci.* **6**, 206–211
6. Nakanishi, Y., Matsuda, N., Aizawa, K., Kashiyama, T., Yamamoto, K., Mimura, T., Ikeda, M., and Maeshima, M. (1999) Molecular cloning of the cDNA for vacuolar H⁺-pyrophosphatase from *Chara corallina*. *Biochim. Biophys. Acta* **1418**, 245–250
7. Maeshima, M. and Yoshida, S. (1989) Purification and properties of vacuolar membrane proton-translocating inorganic

pyrophosphatase from mung bean. *J. Biol. Chem.* **264**, 20068–20073
8. Scott, D.A., de Souza, W., Benchimol, M., Zhong, L., Lu, G.G., Moreno, S.N.J., and Docampo, R. (1998) Presence of a plant-like proton-pumping pyrophosphatase in acidocalcisomes of *Trypanosoma cruzi*. *J. Biol. Chem.* **273**, 22151–22158
9. Motta, L.S., da Silva, W.S., Oliveira, D.M.P., de Souza, W., and Machado, E.A. (2004) A new model for proton pumping in animal cells: the role of pyrophosphate. *Insect Biochem. Mol. Biol.* **34**, 19–27
10. Seufferheld, M., Lea, C.R., Vieira, M., Oldfield, E., and Docampo, R. (2004) The H^+-pyrophosphatase of *Rhodospirillum rubrum* is predominantly located in polyphosphate-rich acidocalcisomes. *J. Biol. Chem.* **279**, 51193–51202
11. Seufferheld, M., Vieira, M.C.F., Ruiz, R.A., Rodrigues, C.O., Moreno, S.N., and Docampo, R. (2003) Identification of organelles in bacteria similar to acidocalcisomes of unicellular eukaryotes. *J. Biol. Chem.* **278**, 29971–29978
12. Belogurov, G.A., Turkina, M.V., Penttinen, A., Huopalahti, S., Baykov, A.A., and Lahti, R. (2002) H^+-pyrophosphatase of *Rhodospirillum rubrum*: high yield expression in *Escherichia coli* and identification of the Cys residues responsible for inactivation by mersalyl. *J. Biol. Chem.* **277**, 22209–22214
13. Kim, E.J., Zhen, R.G., and Rea, P.A. (1995) Site-directed mutagenesis of vacuolar H^+-pyrophosphatase: necessity of Cys^{634} for inhibition by maleimides but not catalysis. *J. Biol. Chem.* **270**, 2630–2635
14. Malinen, A.M., Belogurov, G.A., Salminen, M., Baykov, A.A., and Lahti, R. (2004) Elucidating the role of conserved glutamates in H^+-pyrophosphatase of *Rhodospirillum rubrum*. *J. Biol. Chem.* **279**, 26811–26816
15. Mimura, H., Nakanishi, Y., Hirono, M., and Maeshima, M. (2004) Membrane topology of the H^+-pyrophosphatase of *Streptomyces coelicolor* determined by cysteine-scanning mutagenesis. *J. Biol. Chem.* **279**, 35106–35112
16. Nakanishi, Y., Saijo, T., Wada, Y., and Maeshima, M. (2001) Mutagenesis analysis of functional residues in putative substrate-binding site and acidic domains of vacuolar H^+-pyrophosphatase. *J. Biol. Chem.* **276**, 7654–7660
17. Schultz, A. and Baltscheffsky, M. (2003) Properties of mutated *Rhodospirillum rubrum* H^+-pyrophosphatase expressed in *Escherichia coli*. *Biochim. Biophys. Acta* **1607**, 141–151
18. Bentley, S.D., Chater, K.F., Cerdeno-Tarraga, A.M., Challis, G.L., Thomson, N.R., James, K.D., Harris, D.E., Quall, M.A., Kleser, H., Harper, D., Bateman, A., Brown, S., Chandra, G., Chen, C.W., Collins, M., Cronin, A., Fraser, A., Goble, A., Hidalgo, J., Hornsby, T., Howarth, S., Huang, C.H., Kieser, T., Larke, L., Murphy, L., Oliver, K., O'Neil, S., Rabbinowitsch, E., Rajandream, M.A., Rutherford, K., Rutter, S., Seeger, K., Saunders, D., Sharp, S., Squares, R., Squares, S., Taylor, K., Warrant, T., Wietzorrek, A., Woodward, J., Barrell, B.G., Parkhill, J., and Hopwood, D.A. (2002) Complete genome sequence of the model actinomycetes *Streptomyces coelicolor* A3(2). *Nature* **417**, 141–147
19. Lemercier, G., Dutoya, S., Luo, S., Ruiz, F.A., Rodrigues, C.O., Baltz, T., Docampo, R., and Bakalara, N. (2002) A vacuolar-type H^+-pyrophosphatase governs maintenance of functional acidocalcisomes and growth of the insect and mammalian forms of *Trypanosoma brucei*. *J. Biol. Chem.* **277**, 37369–37376
20. Takasu, A., Nakanishi, Y., Yamauchi, T., and Maeshima, M. (1997) Analysis of the substrate binding site and carboxyl terminal region of vacuolar H^+-pyrophosphatase of mung bean with peptide antibodies. *J. Biochem.* **122**, 883–889
21. Nakanishi, Y., Yabe, I., and Maeshima, M. (2003) Patch clamp analysis of H^+ pump expressed in giant yeast vacuoles. *J. Biochem.* **134**, 615–623
22. Péres-Castiñeira, J.R., Lopéz-Marqués, R.L., Losada, M., and Serrano, A. (2001) A thermostable K^+-stimulated vacuolar-type pyrophosphatase from the hyperthermophilic bacterium *Thermotoga maritima*. *FEBS Lett.* **496**, 6–11
23. Drozdowicz, Y.M., Kissinger, J.C., and Rea, P.A. (2000) AVP2, a sequence-divergent, K^+-insensitive H^+-translocating inorganic pyrophosphatase from *Arabidopsis*. *Plant Physiol.* **123**, 353–362
24. Gordon-Weeks, R., Koren'kov, V.D., Steele, S.H., and Leigh, R.A. (1997) Tris is a competitive inhibitor of K^+ activation of the vacuolar H^+-pumping pyrophosphatase. *Plant Physiol.* **114**, 901–905
25. Zhen, R.G., Kim, E.J., and Rea, P.A. (1994) Localization of cytosolically oriented maleimide-reactive domain of vacuolar H^+-pyrophosphatase. *J. Biol. Chem.* **269**, 23342–23350
26. Nyrén, P., Nore, B.F., and Strid, A. (1991) Proton-pumping *N, N′*-dicyclohexylcarbodiimide-sensitive inorganic pyrophosphate synthase from *Rhodospirillum rubrum*: purification, characterization, and reconstitution. *Biochemistry* **30**, 2883–2887
27. Zhen, R.G., Kim, E.J., and Rea, P.A. (1997) Acidic residues necessary for pyrophosphate-energized pumping and inhibition of the vacuolar H^+-pyrophosphatase by *N,N′*-dicyclohexylcarbodiimide. *J. Biol. Chem.* **272**, 22340–22348
28. Hirono, M., Mimura, H., Nakanishi, Y., and Maeshima, M. (2003) Acylspermidine derivatives isolated from a soft coral, *Sinularia* sp., inhibit plant vacuolar H^+-pyrophosphatase. *J. Biochem.* **133**, 811–816
29. Maeshima, M. (1991) H^+-translocating inorganic pyrophosphatase of plant vacuoles: inhibition by Ca^{2+}, stabilization by Mg^{2+} and immunological comparison with other inorganic pyrophosphatases. *Eur. J. Biochem.* **196**, 11–17
30. Drozdowicz, Y.M., Lu, Y.P., Patel, V., Fitz-Gibbon, S., Miller, J.H., and Rea, P.A. (1999) A thermostable vacuolar-type membrane pyrophosphatase from the archaeon *Pyrobaculum aerophilum*: implications for the origins of pyrophosphate-energized pumps. *FEBS Lett.* **460**, 505–512
31. Maeshima, M. (2001) Tonoplast transporters: organization and function. *Annu. Rev. Plant Physiol. Plant Mol. Biol.* **52**, 469–497
32. Maeshima, M., Nakayasu, T., Kawauchi, K., Hirata, H., and Shimmen, T. (1999) Cycloprodigiosin uncouples H^+-pyrophosphatase of plant vacuolar membrane in the presence of chloride ion. *Plant Cell Physiol.* **40**, 439–442
33. Nakanishi, Y. and Maeshima, M. (1998) Molecular cloning of vacuolar H^+-pyrophosphatase and its developmental expression in growing hypocotyls of mung bean. *Plant Physiol.* **116**, 589–597
34. Marchesini, N., Luo, S., Rodrigues, C.O., Moreno, S.N.J., and Docampo, R. (2000) Acidocalcisomes and a vacuolar H^+-pyrophosphatase in malaria parasites. *Biochem. J.* **347**, 243–253
35. Marchesini, N., Ruiz, F.A., Vieira, M., and Docampo, R. (2002) Acidocalcisomes are functionally linked to the contractile vacuole of *Dictyostelium discoideum*. *J. Biol. Chem.* **277**, 8146–8153
36. Rodrigues, C.O., Scott, D.A., and Docampo, R. (1999) Characterization of a vacuolar pyrophosphatase in *Trypanosoma brucei* and its localization to acidocalcisomes. *Mol. Cell. Biol.* **19**, 7712–7723
37. Rohloff, P., Montalvetti, A., and Docampo, R. (2004) Acidocalcisomes and the contractile vacuole complex are involved in osmoregulation in *Trypanosoma cruzi*. *J. Biol. Chem.* **279**, 52270–52281
38. Baltscheffsky, M. (1967) Inorganic pyrophosphate as an energy donor in photosynthetic and respiratory electron transport phosphorylation systems. *Biochem. Biophys. Res. Commun.* **28**, 270–276